Electronic Supplementary Material (ESI) for Polymer Chemistry.

Polymerization-induced Self-Assembly of PVAc-*b*-PVDF block copolymers via RAFT dispersion polymerization of VDF in dimethylcarbonate

*Marc Guerre,[a] Mona Semsarilar,[b] Franck Godiard,[c] Bruno Améduri,[a] Vincent Ladmiral[†]**

[A]Institut Charles Gerhardt Montpellier UMR5253 CNRS-UM-ENSCM – Equipe Ingénierie et Architectures Macromoléculaires, ENSCM 8, rue de l'école normale, 34296 cedex 5, Montpellier, France.
[b]Institut Européen des Membranes, IEM, UMR-5635, Université de Montpellier, ENSCM, CNRS, Place Eugène Bataillon, 34095 Montpellier cedex 5, France.
[C]Service de Microscopie Electronique, Université de Montpellier, Place Eugène Bataillon, 34095 Montpellier cedex 5, France.

SUPPORTING INFORMATION

Equations used to determine the degree of polymerization and molar masses of PVAc macro-CTAs

$$(S1)\ DP_{\mathrm{PVAc}} = \frac{\int_{4.76}^{5.14} CH(OAc) + \frac{1}{2}\int_{3.18}^{3.51} -CH_2 - XA + \frac{1}{2}\int_{3.95}^{4.13} -CH(OAc) - H + \int_{6.50}^{6.70} -CH(OAc) - XA}{\frac{1}{3}\int_{1.37}^{1.46} -CH_3\ (R-CTA)}$$

$$(S2)\quad M_{n,theo} = \frac{[VAc]_0}{[CTA]_0} \times Yield \times M_{n,VAc} + M_{n,CTAXA}$$

$$(S3)\quad M_{n,PVAc-XA} = M_{n,CTAXA} + DP \times M_{n,VAc}$$

With $M_{\mathrm{n,VAc}}$ = 86.09 g/mol, and $M_{\mathrm{n,\ CTAXA}}$ = 208.29 g/mol.

Equations used to determine the proportions of the polymers chain ends:

1) PVDF:

$$(S4)\ (\%)\ PVDF_T - XA = \frac{\frac{1}{2}\int_{4.02}^{4.17} -CF_2 - CH_2 - XA}{\frac{1}{2}\int_{3.26}^{3.52} -CH_2 - CF_2 - XA + \int_{6.01}^{6.48} -CH_2 - CF_2H + \frac{1}{2}\int_{4.02}^{4.17} -CF_2 - CH_2 - XA + \frac{1}{3}\int_{1.71}^{1.87} -CF_2 - CH_3}$$

$$(S5)\ (\%)\ PVDF_H - XA = \frac{\frac{1}{2}\int_{3.26}^{3.52} -CH_2 - CF_2 - XA}{\frac{1}{2}\int_{3.26}^{3.52} -CH_2 - CF_2 - XA + \int_{6.01}^{6.48} -CH_2 - CF_2H + \frac{1}{2}\int_{4.02}^{4.17} -CF_2 - CH_2 - XA + \frac{1}{3}\int_{1.71}^{1.87} -CF_2 - CH_3}$$

$$(S6)\ (\%)\ PVDF_{H+T} - H = \frac{\int_{6.01}^{6.48} -CH_2 - CF_2H + \frac{1}{3}\int_{1.71}^{1.87} -CF_2 - CH_3}{\frac{1}{2}\int_{3.26}^{3.52} -CH_2 - CF_2 - XA + \int_{6.01}^{6.48} -CH_2 - CF_2H + \frac{1}{2}\int_{4.02}^{4.17} -CF_2 - CH_2 - XA + \frac{1}{3}\int_{1.71}^{1.87} -CF_2 - CH_3}$$

2) PVAc:

$$(S7)\ (\%) - CH(OAc) - CH_2 - XA = \frac{\frac{1}{2}\int_{3.18}^{3.51} -CH(OAc) - CH_2 - XA}{\frac{1}{2}\int_{3.18}^{3.51} -CH(OAc) - CH_2 - XA + \frac{1}{2}\int_{3.95}^{4.13} -CH_2 - (OAc)CH_2 + \int_{6.50}^{6.70} -CH_2 - CH(OAc) - XA}$$

$$(S8)\ (\%) - CH_2 - CH(OAc) - XA = \frac{\int_{6.50}^{6.70} -CH_2 - CH(OAc) - XA}{\frac{1}{2}\int_{3.18}^{3.51} -CH(OAc) - CH_2 - XA + \frac{1}{2}\int_{3.95}^{4.13} -CH_2 - (OAc)CH_2 + \int_{6.50}^{6.70} -CH_2 - CH(OAc) - XA}$$

$$(S9)\ (\%) - CH_2 - (OAc)CH_2 = \frac{\frac{1}{2}\int_{3.95}^{4.13} -CH_2 - (OAc)CH_2}{\frac{1}{2}\int_{3.18}^{3.51} -CH(OAc) - CH_2 - XA + \frac{1}{2}\int_{3.95}^{4.13} -CH_2 - (OAc)CH_2 + \int_{6.50}^{6.70} -CH_2 - CH(OAc) - XA}$$

Run	$PVAc_x$-*b*-$PVDF_y$ X/Y (precipitated BCP)	wt. % (PVAc/PVDF) crude	mol % (PVAc/PVDF) crude	wt. % (PVAc/PVDF) precipitated
2	18/18	85/15	79/21	57/43
3	18/78	51/49	59/41	24/76
4	18/145	31/69	23/77	14/86
5	18/257	16/84	12/88	9/91
7	115/502	55/45	52/48	24/86
9	96/205	74/26	67/33	39/61
10	96/303	57/43	48/52	30/70
11	96/442	36/64	29/71	22/78

Table S1. Weight and molar fractions of crude and precipitated PVAc-*b*-PVDF BCPs.

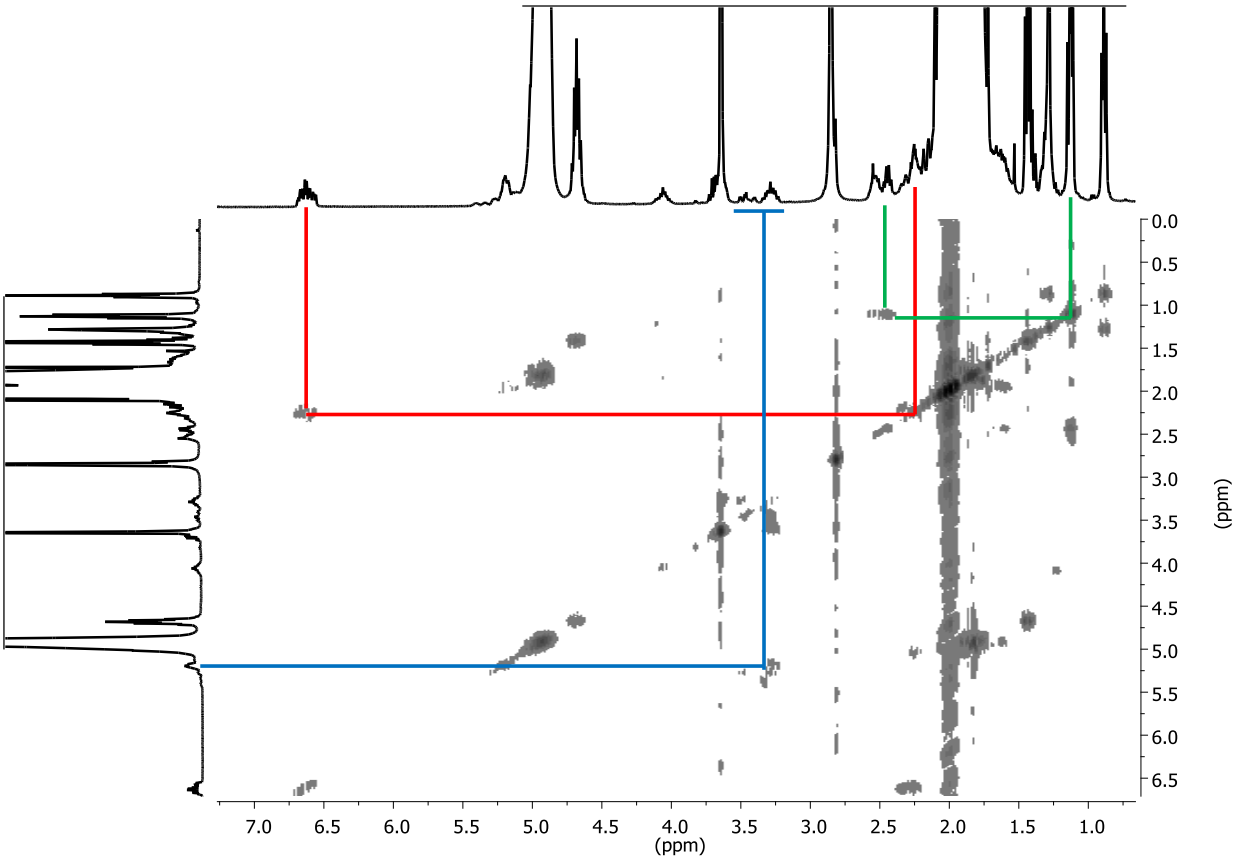

Figure S1. COSY ^{1}H-^{1}H NMR spectrum in $(CD_3)_2CO$ of $PVAc_{18}$-XA synthesized by RAFT polymerization (run 1 Table 1). The red line shows the -**CH$_2$**-(CH_3(C=O)O**CH**-XA correlation ($PVAc_H$-XA); the blue line shows the -**CH(**O(C=O)CH_3)-**CH$_2$**-XA correlation ($PVAc_T$-XA); the green line shows the CH_3O(C=O)(**CH$_3$**)**CH**- correlation (α chain end).

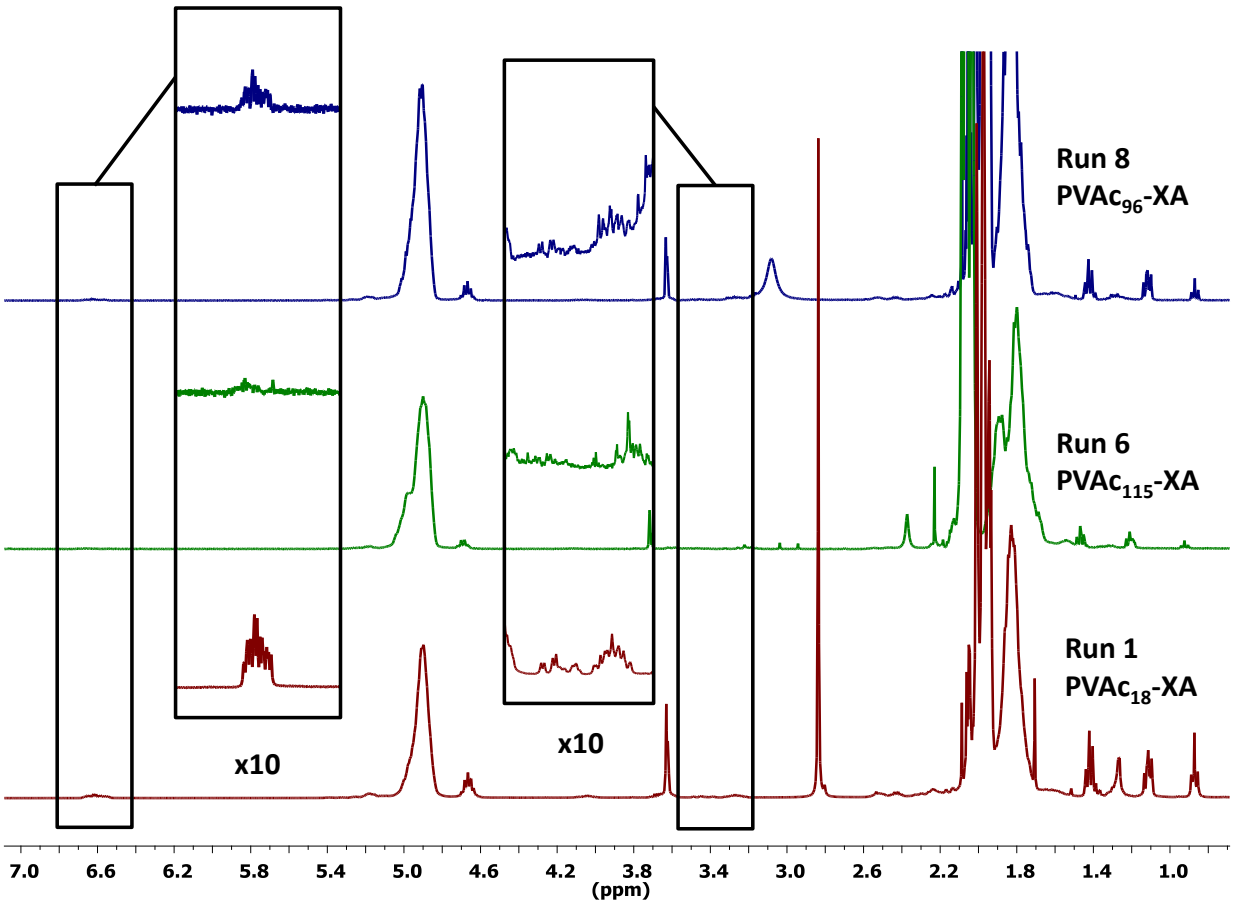

Figure S2. ^{1}H NMR spectrum in $(CD_3)_2CO$ of $PVAc_{18}$-XA (red, bottom, run 1 Table 1), $PVAc_{115}$-XA (green, middle, run 6 Table 1), $PVAc_{96}$-XA (blue, top, run 8 Table 1), synthesized by RAFT polymerization.

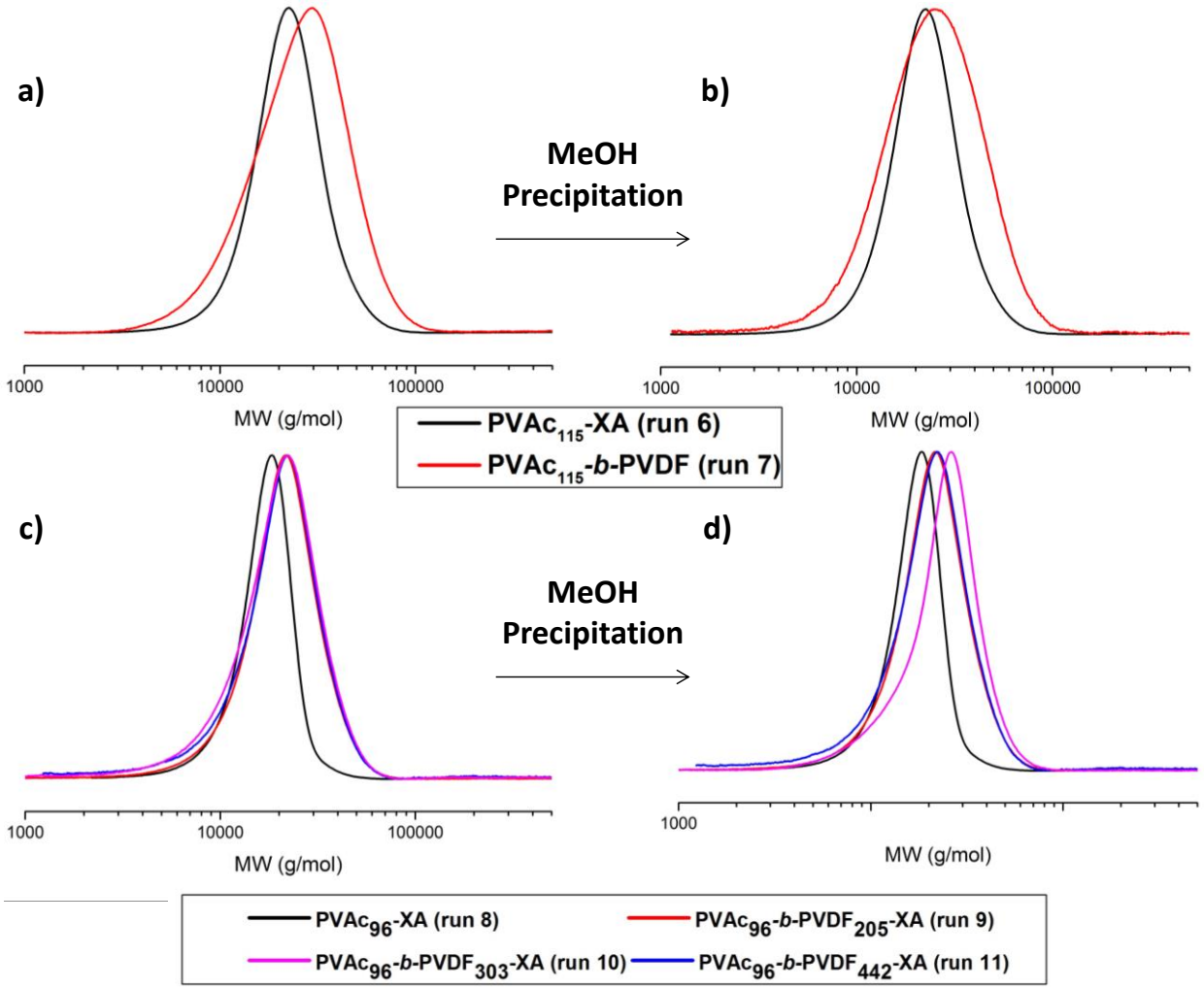

Figure S3. Normalized SEC traces (viscosimetric detector) of: a) $PVAc_{115}$-XA and crude $PVAc_{115}$-*b*-PVDF BCP; b) $PVAc_{115}$-XA and $PVAc_{115}$-*b*-PVDF BCP precipitated in methanol; c) $PVAc_{96}$-XA and crude $PVAc_{96}$-*b*-PVDF BCP; and d) $PVAc_{96}$-XA and $PVAc_{96}$-*b*-PVDF BCP precipitated in methanol.

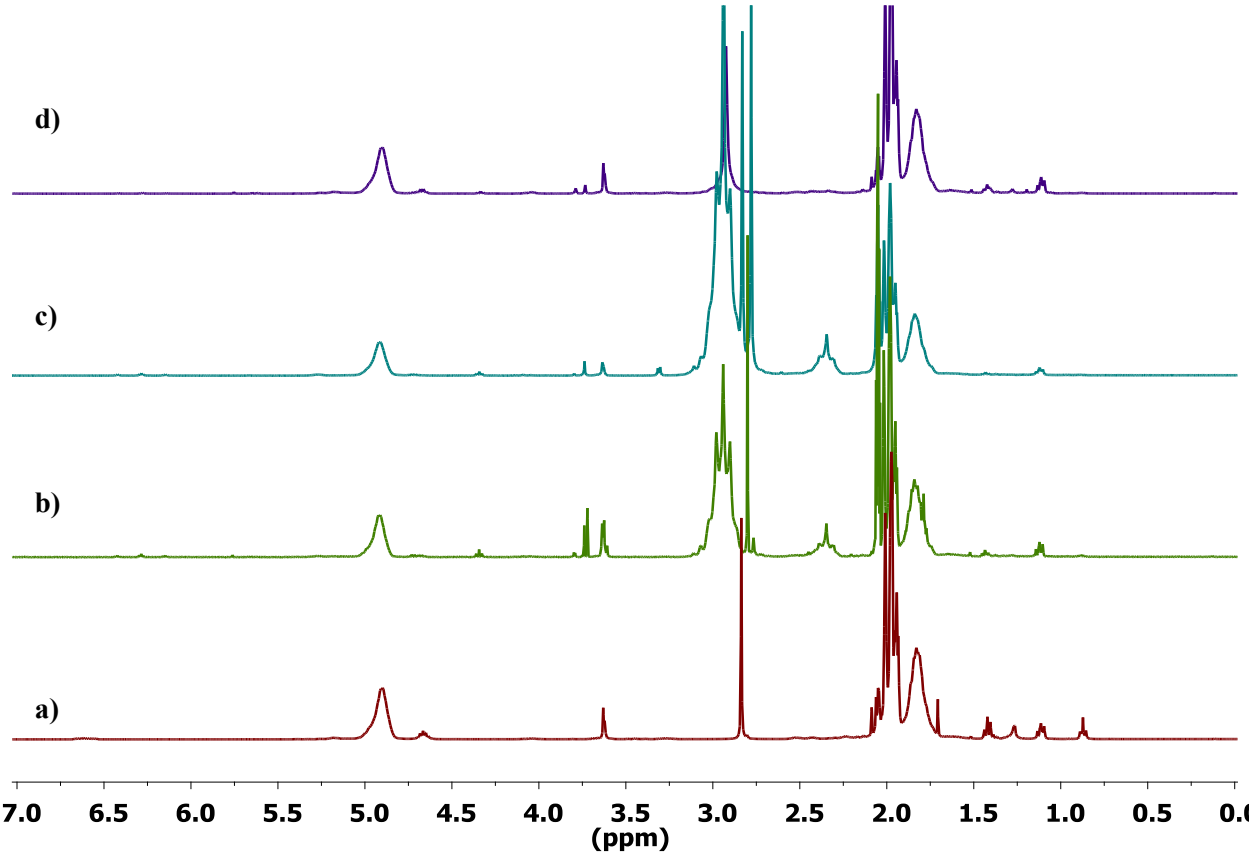

Figure S4. Full ^{1}H NMR spectra in $(CD_3)_2CO$ of a) $PVAc_{18}$-XA (run 1, Table 1), b) $PVAc_{18}$-*b*-$PVDF_{78}$ crude c) $PVAc_{18}$-*b*-$PVDF_{78}$ precipitated in methanol (d) the methanol soluble fraction resulting from the precipitation of $PVAc_{18}$-*b*-$PVDF_{78}$ in cold methanol.

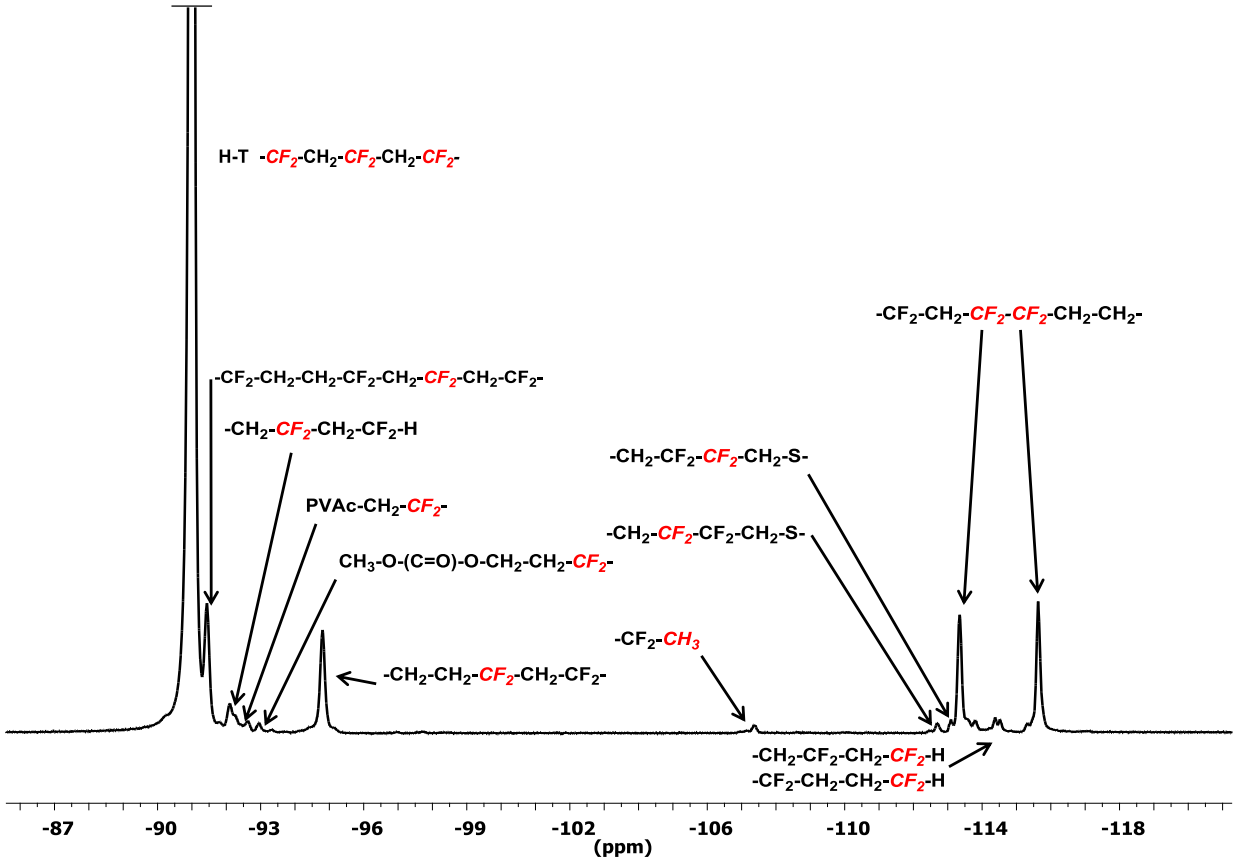

Figure S5. ^{19}F NMR spectrum in $(CD_3)_2CO$ of precipitated $PVAc_{18}$-*b*-$PVDF_{78}$ BCP (run 3, Table 1).

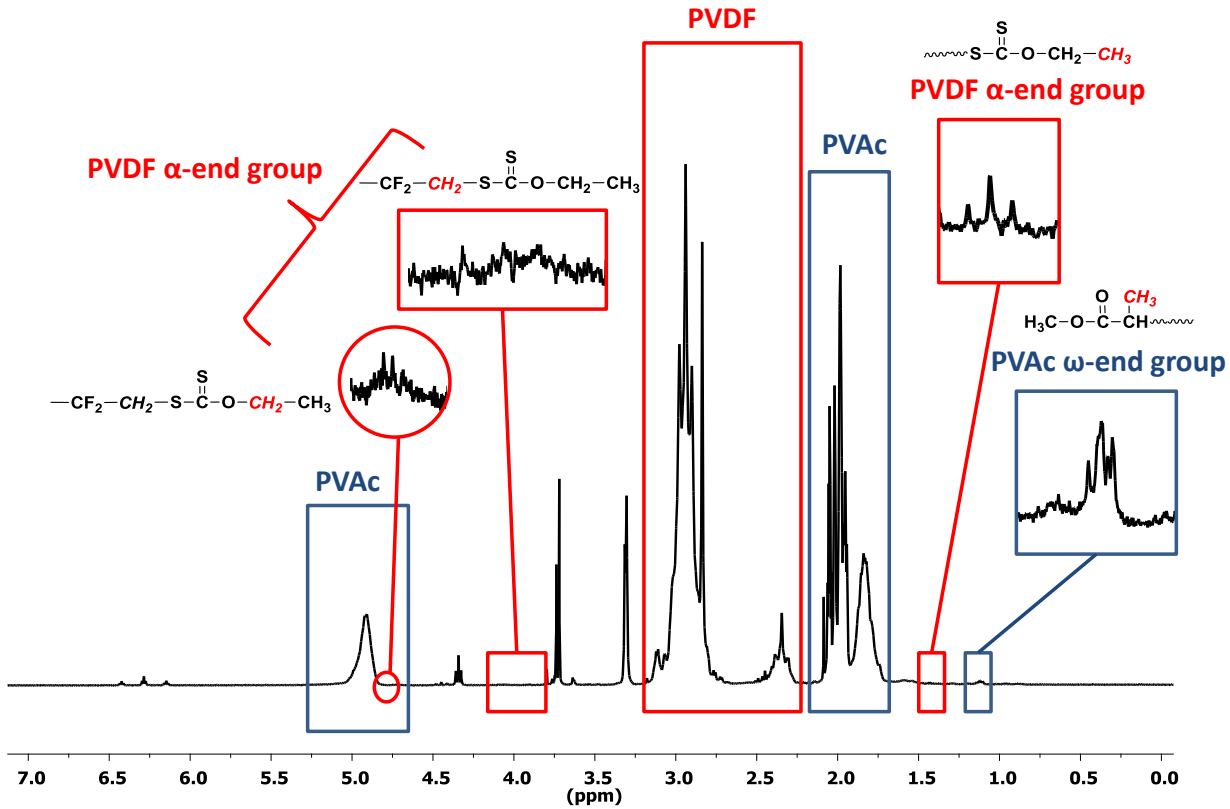

Figure S6. ^{1}H NMR spectrum in $(CD_3)_2CO$ of precipitated $PVAc_{115}$-*b*-$PVDF_{502}$ BCP (run 7, Table 1).

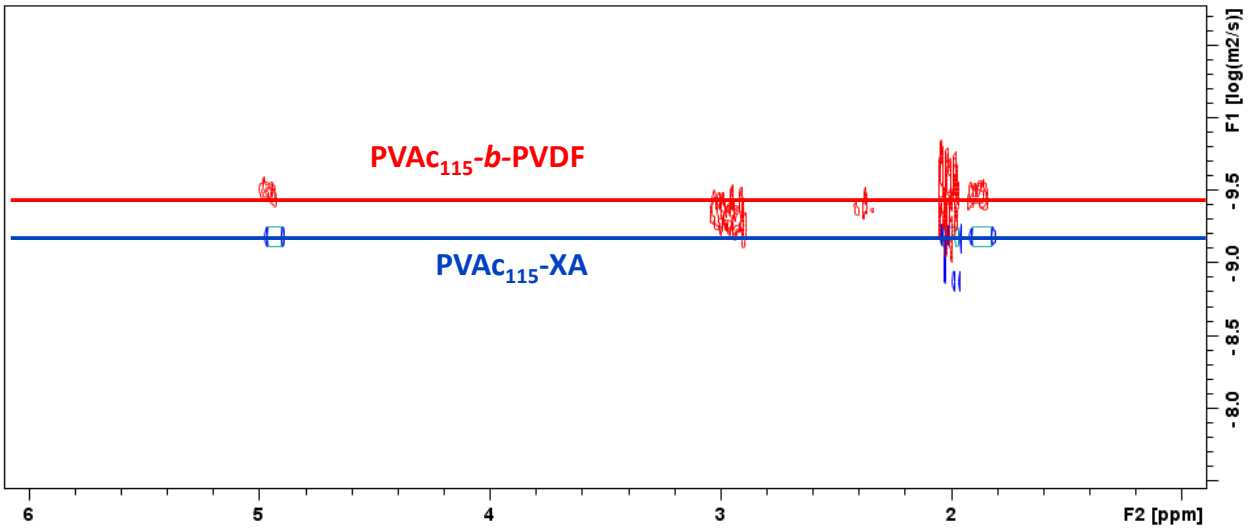

Figure S7. Superposed ^{1}H NMR DOSY spectra in $(CD_3)_2CO$ of $PVAc_{115}$-XA (run 6, Table 1, blue signal) and $PVAc_{115}$-*b*-$PVDF_{502}$ BCP (run 7, Table 1, red signal).

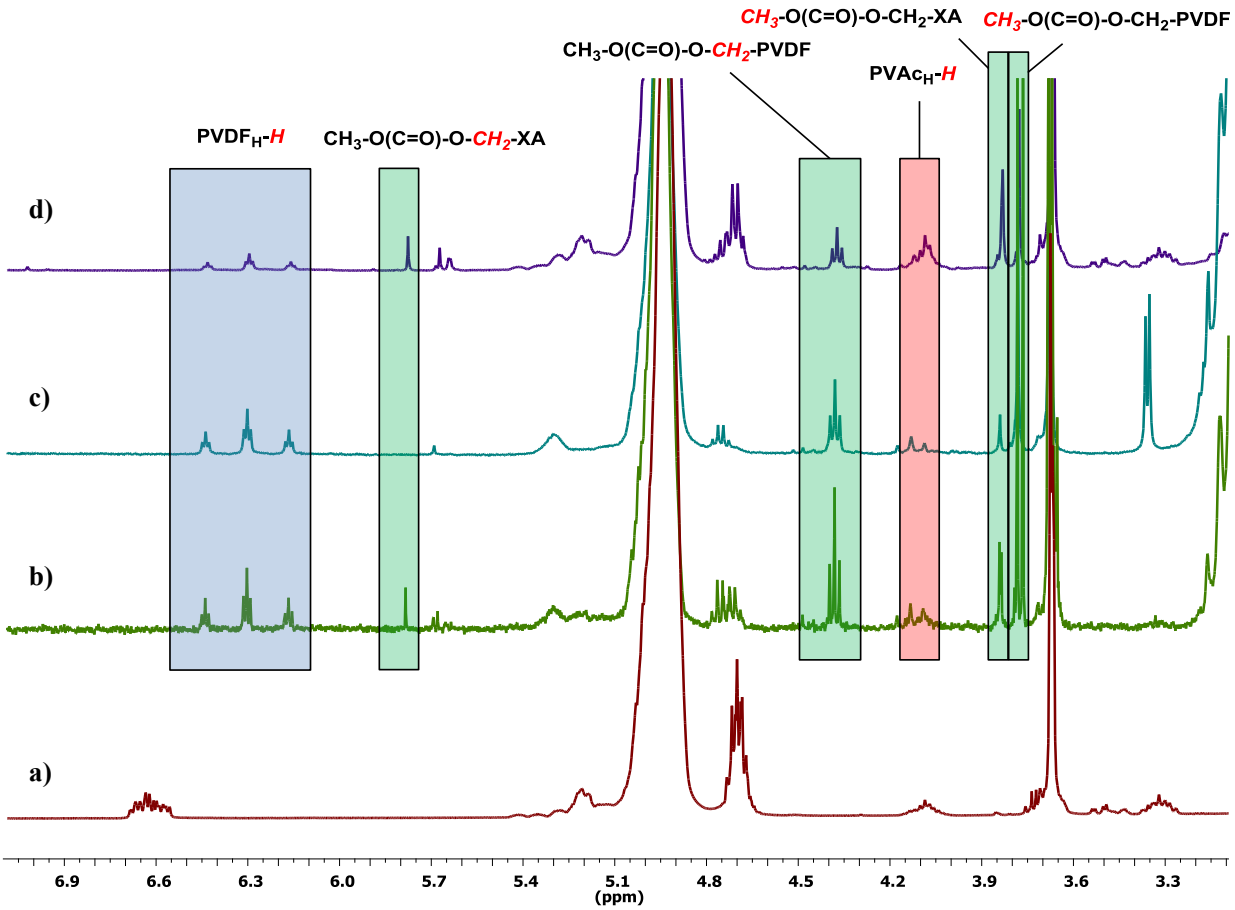

Figure S8. Expansion of the 3.05 to 7.1 ppm region of the ^{1}H NMR spectra in $(CD_3)_2CO$ of a) $PVAc_{18}$-XA (run 1, Table 1), b) Crude $PVAc_{18}$-*b*-$PVDF_{78}$ (run 3, Table 1) c) $PVAc_{18}$-*b*-$PVDF_{78}$ (run 3, Table 1) precipitated in methanol (d) the methanol soluble fraction resulting from the precipitation of $PVAc_{18}$-*b*-$PVDF_{78}$ (run 3, Table 1) in cold methanol.

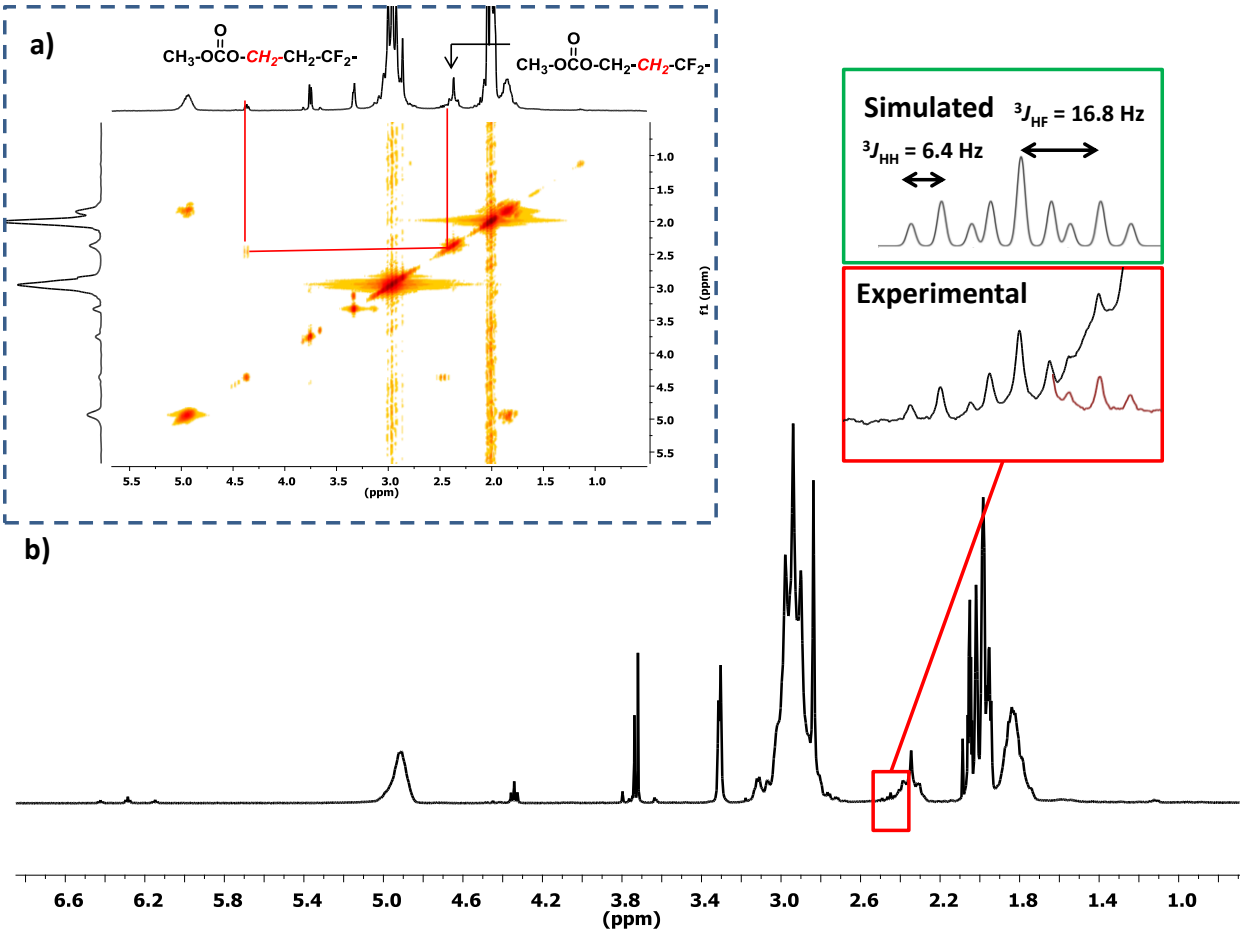

Figure S9. a) COSY ^{1}H-^{1}H NMR spectrum in $(CD_3)_2CO$ of precipitated $PVAc_{115}$-*b*-$PVDF_{502}$ BCP (run 7, Table 1). The red lines highlight the correlation between the -CH_2- group of DMC and the CH_2 of the first added VDF unit in PVDF chains initiated by DMC b) ^{1}H NMR spectrum in $(CD_3)_2CO$ of precipitated $PVAc_{115}$-*b*-PVDF BCP (run 7, Table 1). The expansion of the signals at 2.35-2.55 ppm (red box) shows the experimental pattern (with the expected symmetry drawn in red) of ($CH_3OC(O)$-O-CH_2-**CH_2**-CF_2- protons and the associated simulated pattern.

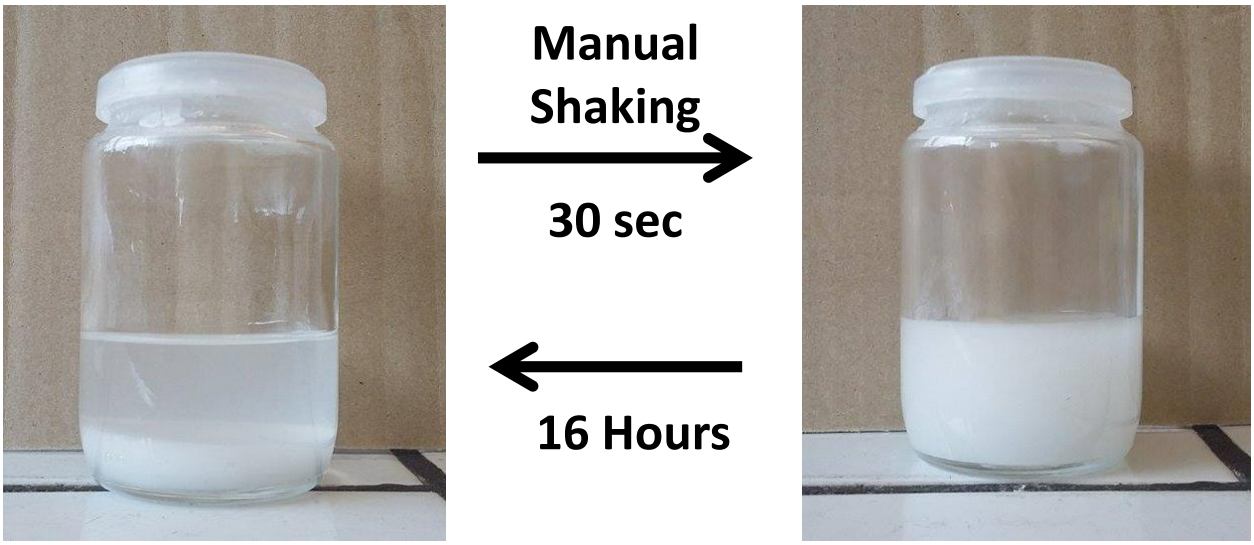

Figure S10. Macroscopic aspect of $PVAc_{18}$-*b*-$PVDF_{257}$ dispersion in DMC (run 5) before and after shaking.

a)

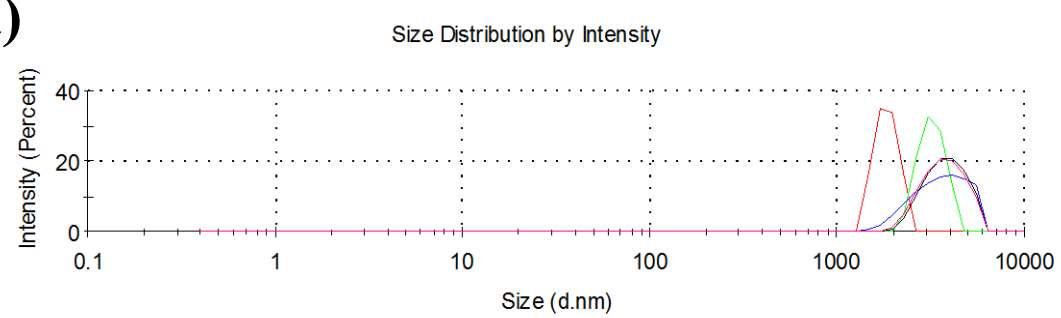
Size Distribution by Intensity
Intensity (Percent)
40
20
0
0.1
1
10
100
1000
10000
Size (d.nm)

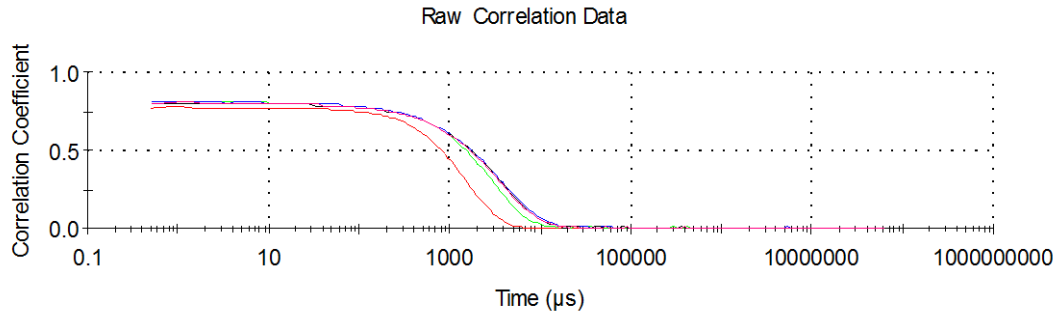
Raw Correlation Data
Correlation Coefficient
1.0
0.5
0.0
0.1
10
1000
100000
10000000
1000000000
Time (µs)

b)

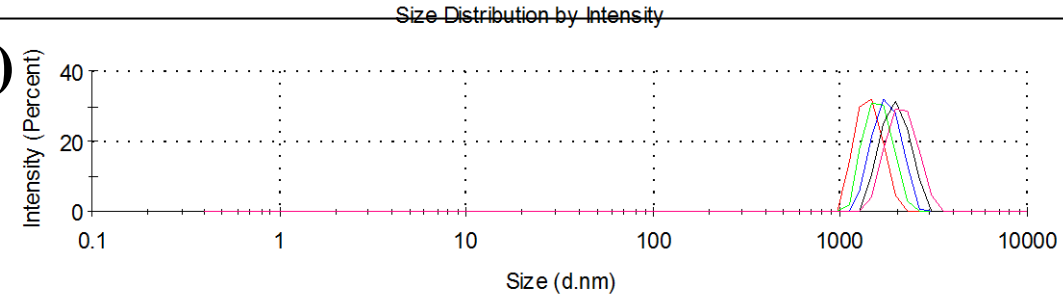
Size Distribution by Intensity
Intensity (Percent)
40
20
0
0.1
1
10
100
1000
10000
Size (d.nm)

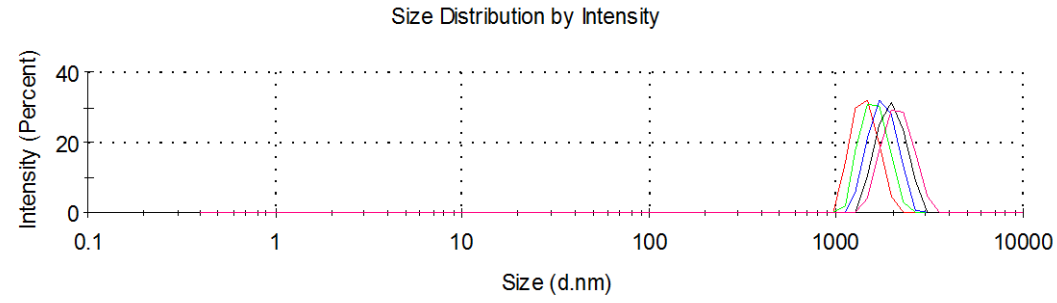
Size Distribution by Intensity
Intensity (Percent)
40
20
0
0.1
1
10
100
1000
10000
Size (d.nm)

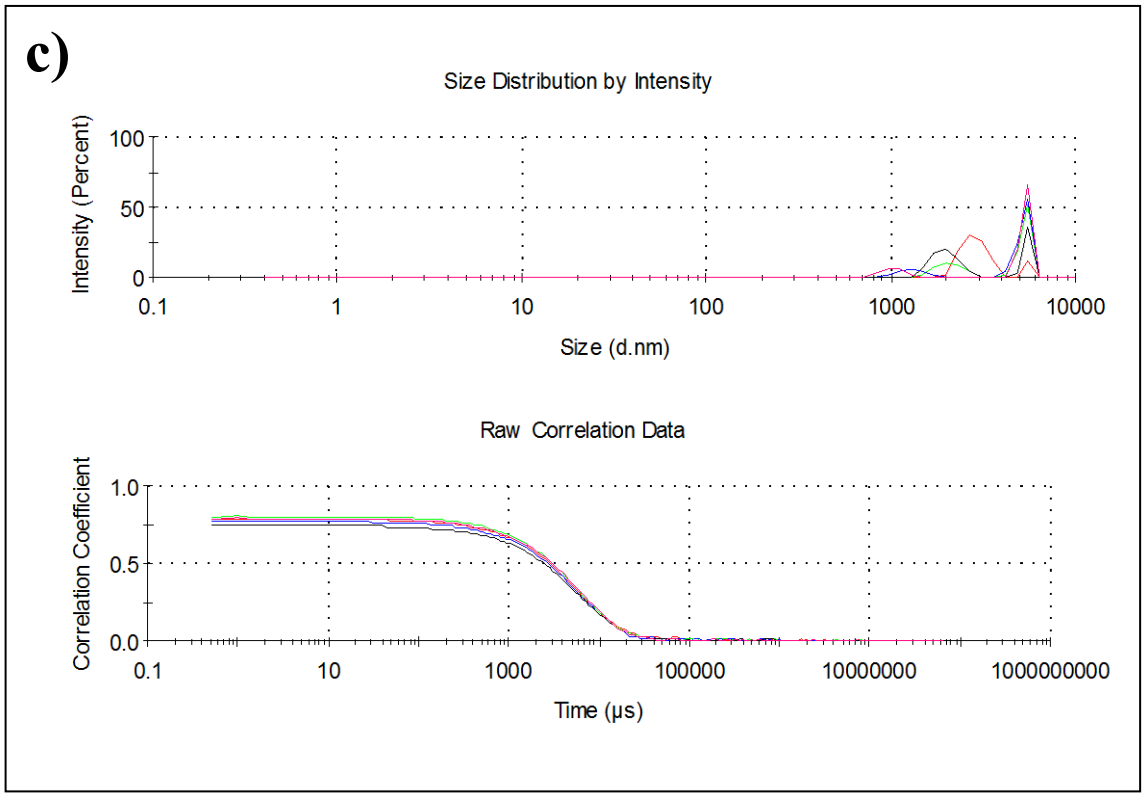

Figure S11. Intensity-average diameter distribution and correlation curve of: a) $PVAc_{18}$-*b*-$PVDF_{18}$ (run 2, Table 1), b) $PVAc_{18}$-*b*-$PVDF_{257}$ (run 5, Table 1) and c) $PVAc_{96}$-*b*-$PVDF_{205}$ (run 9, Table 1) BCPs dispersed in dimethylcarbonate at 1 wt. %.

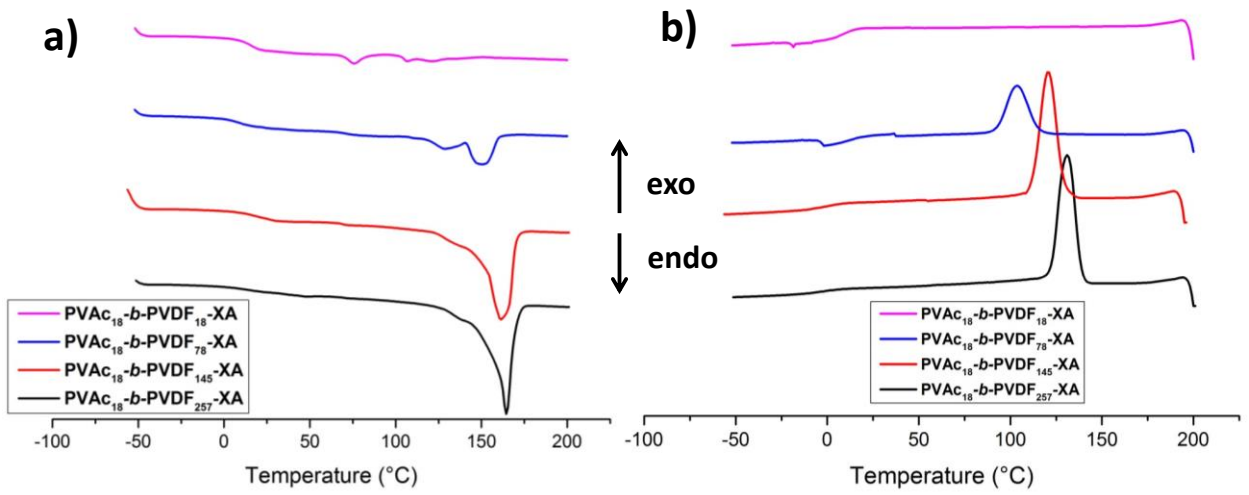

Figure S12. DSC thermograms first heating a) followed by cooling b) of PVAc-*b*-PVDF dried dispersions: $PVAc_{18}$-*b*-$PVDF_{257}$ (black), $PVAc_{18}$-*b*-$PVDF_{145}$ (red) $PVAc_{18}$-*b*-$PVDF_{78}$ (blue) and $PVAc_{18}$-*b*-$PVDF_{18}$ (pink).

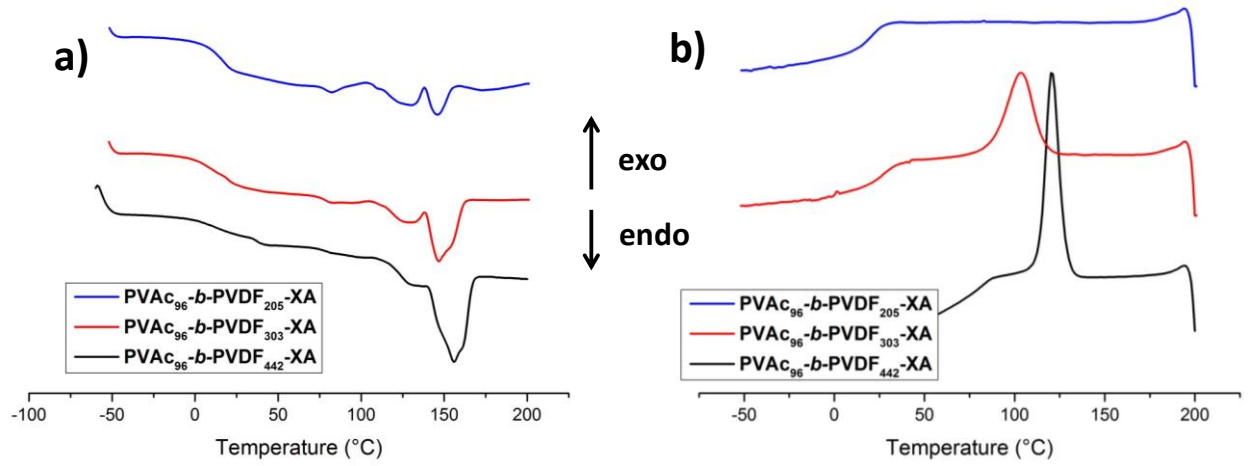

Figure S13. DSC thermograms first heating a) followed by cooling b) of PVAc-*b*-PVDF dried dispersion: $PVAc_{96}$-*b*-$PVDF_{442}$ (black), $PVAc_{96}$-*b*-$PVDF_{303}$ (red) and $PVAc_{18}$-*b*-$PVDF_{205}$ (blue).

Run	X_c (%)	$PVAc_x$-*b*-$PVDF_y$ X/Y	wt. % (PVAc/PVDF) crude
2	33	18/18	85/15
3	45	18/78	51/49
4	81	18/145	31/69
5	64	18/257	16/84
9	42	96/205	74/26
10	51	96/303	57/43
11	52	96/442	36/64

Table S2. Degree of crystallinity (X_c) of the PVDF fraction in the BCPs dispersions determined using equations S9 and S10:

$$X_c(\%) = \frac{\Delta H_f}{\Delta H_f^0 \Phi_m} \times 100 \qquad (S10)$$

With $\Delta H_f^0 \Phi_m$ is a heat of fusion of 100 % crystalline PVDF (104.6 $J.g^{-1}$) and Φ_m is the weight fraction of PVDF.[1,2]

References:

1. K. Nakagawa, Y. Ishida, *J. Polym. Sci. Part B*, 1973, **11**, 2153.
2. J. N. Martins, T. S. Bassano, R. V. B. Oliveira, *Materials Science and Engineering C*, 2012, **32**, 146-151.